HAL
open science

Two-colour generation in a chirped seeded free-electron laser: a close look

Benoît Mahieu, Enrico Allaria, Davide Castronovo, Miltcho Boyanov Danailov, Alexander Demidovich, Giovanni de Ninno, Simone Di Mitri, William M Fawley, Eugenio Ferrari, Lars Fröhlich, et al.

To cite this version:

Benoît Mahieu, Enrico Allaria, Davide Castronovo, Miltcho Boyanov Danailov, Alexander Demidovich, et al.. Two-colour generation in a chirped seeded free-electron laser: a close look. Optics Express, 2013, 21 (19), pp.22728-22741. 10.1364/OE.21.022728 . hal-01859801

HAL Id: hal-01859801

https://hal.science/hal-01859801v1

Submitted on 22 Aug 2018

HAL is a multi-disciplinary open access archive for the deposit and dissemination of scientific research documents, whether they are published or not. The documents may come from teaching and research institutions in France or abroad, or from public or private research centers.

L'archive ouverte pluridisciplinaire **HAL**, est destinée au dépôt et à la diffusion de documents scientifiques de niveau recherche, publiés ou non, émanant des établissements d'enseignement et de recherche français ou étrangers, des laboratoires publics ou privés.

Two-colour generation in a chirped seeded free-electron laser: a close look

Benoît Mahieu,[1,2,3,*] Enrico Allaria,[1] Davide Castronovo,[1] Miltcho B. Danailov,[1] Alexander Demidovich,[1] Giovanni De Ninno,[3,1] Simone Di Mitri,[1] William M. Fawley,[1] Eugenio Ferrari,[1] Lars Fröhlich,[1] David Gauthier,[1,3] Luca Giannessi,[1,4] Nicola Mahne,[1] Giuseppe Penco,[1] Lorenzo Raimondi,[1] Simone Spampinati,[1] Carlo Spezzani,[1] Cristian Svetina,[1,5] Mauro Trovò,[1] and Marco Zangrando[1,6]

[1]*Elettra - Sincrotrone Trieste, S.S.14 - km 163.5 in AREA Science Park, 34149 Basovizza, Italy*
[2]*Service des Photons Atomes et Molécules, Commissariat à l'Energie Atomique, Centre d'Etudes de Saclay, Bâtiment 522, 91191 Gif-sur-Yvette, France*
[3]*Laboratory of Quantum Optics, University of Nova Gorica, Vipavska 11c, 5270 Ajdovščina, Slovenia*
[4]*Theory Group - ENEA C.R. Frascati, Via E. Fermi 45, 00044 Frascati, Italy*
[5]*University of Trieste, Graduate School of Nanotechnology, Piazzale Europa 1, 34127 Trieste, Italy*
[6]*IOM-CNR, S.S.14 - km 163.5 in AREA Science Park, 34149 Basovizza, Italy*
[*]*benoit.mahieu@ensta-paritech.fr*

Abstract: We present the experimental demonstration of a method for generating two spectrally and temporally separated pulses by an externally seeded, single-pass free-electron laser operating in the extreme-ultraviolet spectral range. Our results, collected on the FERMI@Elettra facility and confirmed by numerical simulations, demonstrate the possibility of controlling both the spectral and temporal features of the generated pulses. A free-electron laser operated in this mode becomes a suitable light source for jitter-free, two-colour pump-probe experiments.

© 2013 Optical Society of America

OCIS codes: (140.2600) Lasers and laser optics, Free-electron lasers (FELs); (320.1590) Ultrafast optics, Chirping; (320.5540) Ultrafast optics, Pulse shaping

References and links

1. A. Berni and W. Gregg, "On the utility of chirp modulation for digital signaling," IEEE Transactions on Communications **21**, 748–751 (1973).
2. D. Mihovilovic and R. N. Bracewell, "Adaptive chirplet representation of signals in the timefrequency plane," Electronics Letters **27**, 1159–1161 (1991).
3. R. Szipcs, K. Ferencz, C. Spielmann, and F. Krausz, "Chirped multilayer coatings for broad-band dispersion control in femtosecond lasers," Opt. Lett. **19**, 201–203 (1994).
4. D. Strickland and G. Mourou, "Compression of amplified chirped optical pulses," Opt. Commun. **55**, 447–449 (1985).
5. L. H. Yu, E. Johnson, D. Li, and D. Umstadter, "Femtosecond free-electron laser by chirped pulse amplification," Phys. Rev. E **49**, 4480 (1994).
6. F. Frassetto, L. Giannessi, and L. Poletto, "Compression of XUV FEL pulses in the few-femtosecond regime," Nucl. Instr. and Meth. A **593**, 14–16 (2008).
7. C. Feng, L. Shen, M. Zhang, D. Wang, D. Zhao, and D. Xiang, "Chirped-pulse amplification in a seeded free-electron laser for generating high-power ultra-short radiation," Nucl. Instr. and Meth. A **712**, 113–119 (2013).
8. L. H. Yu, "Generation of intense UV radiation by subharmonically seeded single-pass free-electron lasers," Phys. Rev. A **44**, 5178 (1991).

#191851 - $15.00 USD Received 6 Jun 2013; revised 19 Aug 2013; accepted 20 Aug 2013; published 19 Sep 2013

9. A. A. Lutman, R. Coffee, Y. Ding, Z. Huang, J. Krzywinski, T. Maxwell, M. Messerschmidt, and H.-D. Nuhn, "Experimental demonstration of femtosecond two-color X-ray free-electron laser," Phys. Rev. Lett. **110**, 134801 (2013).
10. V. Petrillo, M. P. Anania, M. Artioli, A. Bacci, M. Bellaveglia, E. Chiadroni, A. Cianchi, F. Ciocci, G. Dattoli, D. Di Giovenale, G. Di Pirro, M. Ferrario, G. Gatti, L. Giannessi, A. Mostacci, P. Musumeci, A. Petralia, R. Pompili, M. Quattromini, J. V. Rau, C. Ronsivalle, A. R. Rossi, E. Sabia, C. Vaccarezza, and F. Villa, "Observation of time-domain modulation of free-electron-laser pulses by multipeaked electron-energy spectrum," accepted for publication in Phys. Rev. Lett.
11. E. Allaria, F. Bencivenga, R. Borghes, F. Capotondi, D. Castronovo, P. Charalambous, P. Cinquegrana, M. B. Danailov, G. De Ninno, A. Demidovich, S. Di Mitri, B. Diviacco, D. Fausti, W. M. Fawley, E. Ferrari, L. Froehlich, D. Gauthier, A. Gessini, L. Giannessi, R. Ivanov, M. Kiskinova1, G. Kurdi, B. Mahieu, N. Mahne, I. Nikolov, C. Masciovecchio, E. Pedersoli, G. Penco, L. Raimondi, C. Serpico, P. Sigalotti, S. Spampinati, C. Spezzani, C. Svetina, M. Trovò, and M. Zangrando, "Two-color pump-probe experiment with twin-pulse-seed XUV free electron laser," accepted for publication in Nat. Commun.
12. M. Labat, N. Joly, S. Bielawski, C. Szwaj, C. Bruni, and M. E. Couprie, "Pulse splitting in short wavelength seeded free electron lasers," Phys. Rev. Lett. **103**, 264801 (2009).
13. G. De Ninno, B. Mahieu, E. Allaria, L. Giannessi, and S. Spampinati, "Chirped seeded free-electron lasers: self standing light sources for two-colour pump-probe experiments," Phys. Rev. Lett. **110**, 064801 (2013).
14. C. Svetina, A. Abrami, I. Cudin, C. Fava, S. Gerusina, R. Gobessi, L. Rumiz, G. Sostero, M. Zangrando, and D. Cocco, "Characterization of the FERMI@Elettra's on-line photon energy spectrometer," Proc. SPIE **8139**, 81390J (2011).
15. M. Zangrando, A. Abrami, D. Cocco, C. Fava, S. Gerusina, R. Gobessi, N. Mahne, E. Mazzucco, L. Raimondi, L. Rumiz, C. Svetina, and F. Parmigiani, "The photon beam transport and diagnostics system at FERMI@Elettra, the Italian seeded FEL source: commissioning experience and most recent results," Proc. SPIE **8504**, 850404 (2012).
16. G. De Ninno, E. Allaria, M. Coreno, F. Curbis, M. B. Danailov, E. Karantzoulis, A. Locatelli, T. O. Mente, M. A. Nino, C. Spezzani, and M. Trovò, "Generation of ultrashort coherent vacuum-ultraviolet pulses using electron storage rings: a new bright light source for experiments," Phys. Rev. Lett. **101**, 053902 (2008).
17. E. Allaria, R. Appio, L. Badano, W.A. Barletta, S. Bassanese, S.G. Biedron, A. Borga, E. Busetto, D. Castronovo, P. Cinquegrana, S. Cleva, D. Cocco, M. Cornacchia, P. Craievich, I. Cudin, G. D'Auria, M. Dal Forno, M.B. Danailov, R. De Monte, G. De Ninno, P. Delgiusto, A. Demidovich, S. Di Mitri, B. Diviacco, A. Fabris, R. Fabris, W. Fawley, M. Ferianis, E. Ferrari, S. Ferry, L. Froehlich, P. Furlan, G. Gaio, F. Gelmetti, L. Giannessi, M. Giannini, R. Gobessi, R. Ivanov, E. Karantzoulis, M. Lonza, A. Lutman, B. Mahieu, M. Milloch, S.V. Milton, M. Musardo, I. Nikolov, S. Noe, F. Parmigiani, G. Penco, M. Petronio, L. Pivetta, M. Predonzani, F. Rossi, L. Rumiz, A. Salom, C. Scafuri, C. Serpico, P. Sigalotti, S. Spampinati, C. Spezzani, M. Svandrlik, C. Svetina, S. Tazzari, M. Trovo, R. Umer, A. Vascotto, M. Veronese, R. Visintini, M. Zaccaria, D. Zangrando, and M. Zangrando, "Highly coherent and stable pulses from the FERMI seeded free-electron laser in the extreme ultraviolet," Nat. Photonics **6**, 699–704 (2012).
18. G. Stupakov, "Effect of finite pulse length and laser frequency chirp on HGHG and EEHG seeding," SLAC Report No. SLAC-PUB-14639 (2011).
19. E. Allaria, "FEL commissioning at FERMI@Elettra," talk at Free-Electron Laser Conference 2011, WEOBI1.
20. M. B. Danailov, A. Demidovich, R. Ivanov, I. Nikolov, P. Sigalotti, and P. Cinquegrana, "Design and first experience with the FERMI seed laser," in Proceedings of the Free-Electron Laser Conference 2011, TUOC4.
21. J. C. Diels and W. Rudolph, *Ultrashort Laser Pulse Phenomena* (Academic Press, 2006).
22. S. G. Biedron, S. V. Milton, and H. P. Freund, "Modular approach to achieving the next-generation X-ray light source," Nucl. Instr. and Meth. A, **475**, 401 (2001).
23. T. Shaftan and L. H. Yu, "High-gain harmonic generation free-electron laser with variable wavelength," Phys. Rev. E **71**, 046501 (2005).
24. W. Fawley and G. Penn, "Thoughts on spectral broadening effects in FERMI and other FELs based upon seeded harmonic generation," FERMI Tech. Note ST/F-TN-06/07 (2006).
25. A. A. Lutman, G. Penco, P. Craievich, and J. Wu, "Impact of an initial energy chirp and an initial energy curvature on a seeded free electron laser: the Greens function," J. Phys. A: Math. Theor. **42**, 045202 (2009).
26. A. A. Lutman, G. Penco, P. Craievich, and J. Wu, "Impact of an initial energy chirp and an initial energy curvature on a seeded free electron laser: free electron laser properties," J. Phys. A: Math. Theor. **42**, 085405 (2009).
27. W. Graves, private communication.
28. T. P. Wangler, *RF Linear Accelerators* (Wiley-VCH, 2008).
29. P. Emma, "X-band RF harmonic compensation for linear bunch compression in the LCLS," LCLS-TN-01-1 (2001).
30. J. B. Murphy, S. Krinsky, and R. L. Gluckstern, "Longitudinal wakefield for synchrotron radiation," in Proceedings of the 1995 Particle Accelerator Conference **5**, 2980–2982 (1995).
31. P. Craievich, S. Di Mitri, M. Ferianis, M. Veronese, M. Petronio, and D. Alesini, "A transverse RF deflecting cavity for the FERMI@Elettra project," in Proceedings of DIPAC 2007, TUPC10.

#191851 - $15.00 USD Received 6 Jun 2013; revised 19 Aug 2013; accepted 20 Aug 2013; published 19 Sep 2013
(C) 2013 OSA

32. J. Wu, J. B. Murphy, P. J. Emma, X. Wang, T. Watanabe, and X. Zhong, "Interplay of the chirps and chirped pulse compression in a high-gain seeded free-electron laser," JOSA B **24**, 484–495 (2007).
33. S. Reiche, "GENESIS 1.3: a fully 3D time-dependent FEL simulation code," Nucl. Instr. Meth. A **429**, 243–248 (1999).
34. L. Giannessi, "Overview of Perseo, a system for simulating FEL dynamics in Mathcad," in Proceedings of the Free-Electron Laser Conference 2006, MOPPH026.
35. C. La-O-Vorakiat, E. Turgut, C. A. Teale, H. C. Kapteyn, M. M. Murnane, S. Mathias, M. Aeschlimann, C. M. Schneider, J. M. Shaw, H. T. Nembach, and T. J. Silva, "Ultrafast demagnetization measurements using extreme ultraviolet light: comparison of electronic and magnetic contributions," Phys. Rev. X **2**, 011005 (2012).

Introduction

Chirped pulse modulation is a widely used technique, with relevant applications in several fields of research, ranging from digital communication [1] to radar detection [2], and from optics [3] to laser physics. In a broadband laser, frequency chirping is employed to stretch a short pulse prior to amplification. This stretching and the associated lower intensity mitigates the problem of phase distortion in the amplification medium. After pulse amplification, the pulse is recompressed to recover a short duration and, hence, high power [4]. A similar method has been proposed [5–7] to enhance the power generated by a single-pass seeded free-electron laser (FEL) working in the so-called coherent harmonic generation (CHG) regime [8]. After amplification and removal of the chirp, one in principle can obtain a high power, nearly Fourier-transform-limited pulse.

In this paper, we characterize the performance of a seeded FEL where frequency chirping on the seed laser is instead exploited to generate two independent pulses spectrally and temporally separated in an externally controllable fashion. The generation of multiple pulses of different colours in FEL's is opening new opportunities for pump and probe experiments in spectral regions ranging from vacuum-ultraviolet to hard X-rays with unprecedented brightness. Recently, the LCLS group has reported the generation of pairs of temporally and spectrally separated soft X-ray FEL pulses via a double undulator scheme [9]. Similar studies are ongoing at SPARC [10], where two distinct electron bunches at different energies generate independent pulses of radiation. At FERMI@Elettra, multiple pulses have also been obtained recently with a different technique, based on the simultaneous injection of two different seed pulses on the same electron bunch [11]. In this case the two pulses minimum separation is limited by the seed pulse length. The method we propose here allows to reduce this distance by using a single seed pulse and exploiting saturation to generate the pulse splitting [12, 13].

The paper is divided into the following parts: in Section 1 we introduce the principle upon which a CHG FEL is based, with specific reference to the case of the FERMI@Elettra FEL [17]. We then qualitatively describe the formation of the double spectral peak, when the seed laser carries a linear frequency chirp. In Section 2, we give a description of the effects due to both a laser frequency chirp and an electron beam energy chirp. Then in Section 3, we present the results obtained on the FERMI@Elettra FEL and, in Section 4, compare them to numerical simulations. Finally, we summarize our conclusions and provide some perspectives for future experimental studies.

1. Formation of the spectral double peak

A CHG FEL such as FERMI@Elettra typically employs a layout similar to that shown in Fig. 1. A relativistic electron beam first propagates through the periodic field generated by an undulator, called the modulator, simultaneously interacting with a powerful coherent light source (e.g., a low-order harmonic of a Ti:Sapphire laser). This interaction coherently modulates the electron energy which then leads to a longitudinally-regular charge distribution after the electrons pass through a chromatically-dispersive magnet. Such a spatial modulation, called bunching,

#191851 - $15.00 USD Received 6 Jun 2013; revised 19 Aug 2013; accepted 20 Aug 2013; published 19 Sep 2013
(C) 2013 OSA

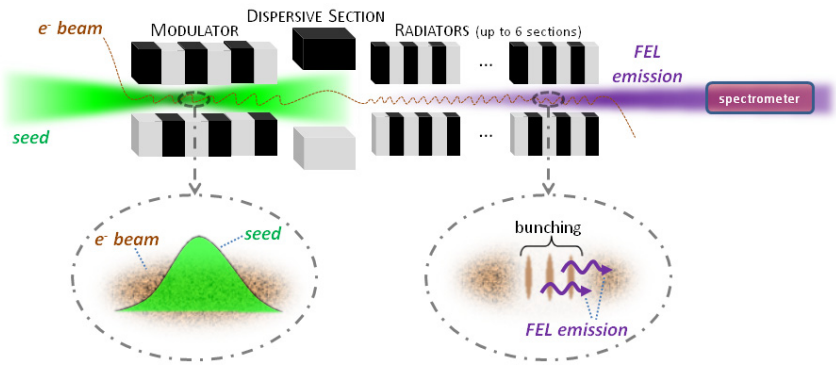

Fig. 1. Schematic layout of the CHG configuration of FERMI@Elettra (see text for details on the FEL process). The output light is separated downstream the FEL line by a grazing-incidence mirror. The fraction corresponding to zeroth order of diffraction ($\geq 95\%$ of the total) is sent to experimental user beamlines, whereas the much weaker, first order component is sent to an online diagnostic spectrometer where it strikes a YAG:Ce crystal, whose visible fluorescence is then measured by a charge-coupled device (CCD) [14, 15]. The spectrometer resolution is about 1.4 meV per CCD pixel.

has nonzero spectral components at both the seed wavelength and at its higher harmonics. After the dispersive section, electron beam enters one or more additional undulators (called the radiators), whose normalized magnetic deflection parameters K are tuned for fundamental FEL resonance to occur at an integral harmonic of the seed wavelength:

$$\lambda_n = \frac{\lambda_s}{n} = \frac{\lambda_u}{2\gamma^2}\,(1+\frac{K^2}{2}). \tag{1}$$

Here λ_s is the seed wavelength, λ_u the radiator period, n the harmonic order and γ the relativistic Lorentz factor characterizing the mean energy of the electron beam.

The resultant FEL radiation, which is highly temporally coherent due to the periodic bunching, can undergo quadratic (low-gain regime) or exponential (high-gain regime) amplification. For a sufficiently long radiator, the FEL process will reach saturation. The main parameters of the FERMI@Elettra configuration relevant for our experimental studies are listed in Table 1 and its caption. One should note that on FERMI@Elettra the seed pulses are much shorter than the electron beam. This is a critical point both for the spectral quality of the FEL emission and the spectro-temporal pulse-splitting phenomenon.

As shown in Fig. 2(a), under conditions of moderate seed power and a temporally flat (i.e, both in energy and current) electron beam, the spectro-temporal properties of CHG mimic those of the seed [16, 17]: starting with a Gaussian seed pulse with a given duration and wavelength λ, one ends up with an output Gaussian CHG pulse at wavelength λ_n with slightly shorter duration [18] . However, this statement (which, in the temporal domain, is mainly a prediction of numerical simulations, due to the lack of temporal diagnostics in the vacuum-ultraviolet spectral range), is true only under certain limits and depends on the regime of operation of the FEL. Indeed, when increasing the seed power, the temporal edges of the seed pulse are also able to produce strong bunching at entrance to the radiator so that a larger part of the electron beam emits intense FEL radiation, giving a longer FEL pulse. For very high seed powers, the electron-beam energy modulation at the peak of the seed (i.e., the central position for a Gaussian) becomes too strong for the particular R_{56} value characterizing the strength of the dispersive section. Then there is an overbunching effect and the resultant bunching in the radiator is

#191851 - $15.00 USD Received 6 Jun 2013; revised 19 Aug 2013; accepted 20 Aug 2013; published 19 Sep 2013
(C) 2013 OSA

Table 1. Parameters of FERMI@Elettra relevant for the experiments reported in this paper. The seed transverse size is defined as the standard deviation of the transverse intensity distribution measured at the modulator entrance. The R_{56} parameter is the momentum compaction factor characterizing the strength of the dispersive section [8]. The undulators were set so as to generate circularly polarized FEL radiation, with a typical energy/pulse of $20\,\mu$J.

Electron beam	Mean energy	≈ 1 GeV
	Peak current	≈ 300 A
	Duration (FWHM)	1.5 ps
	Charge	500 pC
Seed	Central wavelength	261 nm
	Temporal profile	Gaussian
	Duration (FWHM)	≈ 200 fs
	Energy	$10-150\,\mu$J
	Transverse size (RMS)	$\approx 350\,\mu$m
Modulator	Period	100 mm
	Number of periods	32
Dispersive section	R_{56}	$20-50\,\mu$m
Radiators	Number	2
	Harmonic order n	6
	Period	55 mm
	Number of periods	44

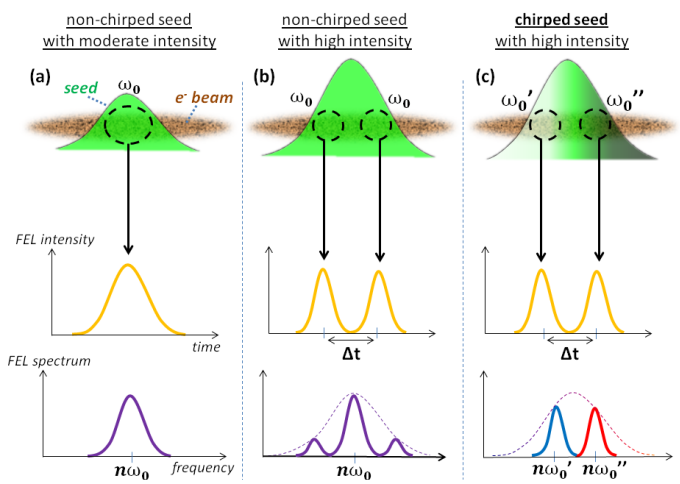

Fig. 2. Sketch of the seed-electrons interaction and resulting FEL (temporal and spectral) outputs for different seed configurations: no chirp and moderate seed intensity (a), no chirp and high seed intensity (b), chirped seed with high intensity (c). In (a), the optimum seed-electrons interaction occurs around the center of the seed pulse so that the FEL output mimics the shape of the seed. In (b), the FEL pulse temporally splits in two because the seed power is too high in the middle of the pulse: a beating between the two sub-pulses involves a frequency modulation but the spectrum remains centered on a single peak at the harmonic n of the constant seed frequency ω_0. In (c), the chirp of the seed combined with the temporal pulse splitting leads to the creation of two separated spectral peaks corresponding to the harmonics of the frequencies ω_0' and ω_0'' at the respective position of each sub-pulse.

#191851 - $15.00 USD Received 6 Jun 2013; revised 19 Aug 2013; accepted 20 Aug 2013; published 19 Sep 2013
(C) 2013 OSA

strongly depressed. Thus, the FEL emission from this central position falls. On the other hand, there are two temporal positions with lower seed power, symmetric with respect to the peak of the seed, that match the optimum bunching condition for a given R_{56}. Accordingly, the FEL signal grows and reaches the maximum intensity in these regions. This scenario is represented in Fig. 2(b). For a sufficiently strong seed intensity, the FEL power at the central position almost vanishes and two successive pulses appear, as previously described in [12]. This phenomenon becomes particularly interesting if the seed is chirped i.e., if its frequency depends on the longitudinal position. As shown in Fig. 2(c), in this situation the split temporal pulses have also different frequencies. In other words, two independent pulses with two different frequencies are created [13].

Two-colour pulse generation by a seeded FEL was observed for the first time [19] early in 2011 during the commissioning of FERMI@Elettra. A typical measurement of the FEL spectrum as a function of the seed power is shown in Fig. 3. By increasing the seed energy, the portion of electrons getting over-bunched increases, leading to a larger separation of the spectral peaks. As shown in the Fig. insets, the two-colour spectra are very stable on a shot-to-shot basis with very good repeatability. We obtained very similar pulse-splitting results by increasing the strength of the dispersive section while keeping the seed power constant (this is illustrated later in Fig. 7(a)).

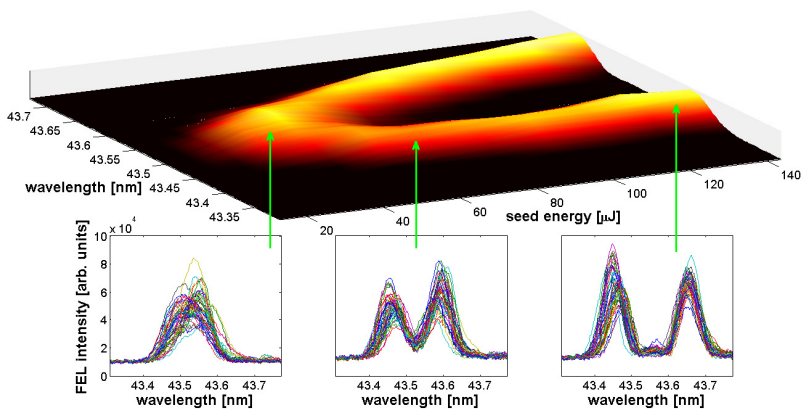

Fig. 3. Experimental characterization of the spectral separation between FEL peaks, as a function of seed energy per pulse. The insets show the spectrum of fifty consecutive shots, integrated at the positions indicated by the arrows on the projected Fig. (higher part).

The spectro-temporal properties of the FEL emission are also affected by the quality of the electron beam. In particular, effects due to an energy chirp (i.e., the mean electron energy varies with longitudinal position) can couple with those from the frequency chirp carried by the seed laser. This interplay may have an impact on the process of formation of the two peaks, as well as on their spectral and temporal separations. In order to better explain the process of production of the double peak, we will now provide a description of the seed laser and electron beam chirps, with particular reference to the case of FERMI@Elettra.

2. Description of seed and electron beam chirps

Seed pulse: frequency chirp

The seed pulse used at FERMI@Elettra is the third harmonic of a Ti:Sapphire laser; both the temporal and spectral profiles are well fit by a Gaussian dependence [20]. The presence of a

#191851 - $15.00 USD Received 6 Jun 2013; revised 19 Aug 2013; accepted 20 Aug 2013; published 19 Sep 2013
(C) 2013 OSA

linear frequency chirp can be modelled by a quadratic term in the phase of the laser electric field:

$$E(t) = A(t)e^{i(\omega_0 t + \Gamma_i t^2)}. \tag{2}$$

Here A(t) stands for the temporal envelope while the exponential term carries the phase of the oscillations, including the rapidly-oscillating term at the central angular frequency ω_0 and the quadratic term $\Gamma_i t^2$. The parameter Γ_i is given by:

$$\Gamma_i = \pm \frac{1}{4\sigma_t^2}\sqrt{4\sigma_t^2\sigma_\omega^2 - 1}, \tag{3}$$

σ_t and σ_ω being the standard deviations of the temporal intensity profile and the spectrum, respectively. The sign of Γ_i corresponds to the sign of the induced frequency dispersion. In the setup adopted at FERMI@Elettra, the frequency dispersion of the seed pulse may be controlled in three different (but eventually combined) ways: (1) by propagation of the seed through different materials; (2) by passage through a dedicated set of gratings; and (3) by increasing the seed intensity, which causes self-phase modulation [21]. It is worth noting that in the presence of self-phase modulation, the chirp cannot be considered as being linear at or near the edges of the pulse. Moreover, the self-modulation process is associated with a spectral broadening. This broadening has been measured and taken into account in the present study. We also note that, for the experiments reported in this paper, the Gaussian shape of the pulse is preserved over the full range of seed energies.

The instantaneous frequency of the pulse is the derivative of the temporal phase (see Eq. 2):

$$\omega(t) = \omega_0 + 2\Gamma_i t. \tag{4}$$

Positive Γ_i's define a positive linear chirp; i.e., smaller frequencies (longer wavelengths) arrive first. On the contrary, negative chirps arise for negative Γ_i values. In both cases, two parts of the pulse separated by a duration Δt have different frequencies, whose separation is, according to Eq. 4:

$$\Delta\omega(\Delta t) = 2\Gamma_i \Delta t. \tag{5}$$

For a CHG FEL that operates in the pulse splitting regime, with the radiators tuned at the harmonic n and the two sub-pulses separated by Δt, we thus expect the frequency separation between the two spectral peaks to be:

$$\Delta\omega_n = n\Delta\omega \tag{6}$$

For the sake of convenience, in the reminder of this paper, we will speak in terms of wavelength λ, instead of angular frequency ω and will therefore consider $\Delta\lambda_n$ as the spectral separation of the two peaks of the FEL emission.

For a given spectral bandwidth, the presence of chirp in the seed pulse will increase its temporal duration. At two positions separated by $4\sigma_t$ and symmetric with respect to the center of the pulse, the electron bunch experiences 13.5% of the maximum intensity of a Gaussian profile seed. For our seed laser parameters, efficient seeding seems difficult below 10% of the peak intensity, i.e., on the very far edges of the seed pulse. Therefore, we may consider $4\sigma_t$ as the maximum practically achievable Δt for a given chirp. Figure 4 displays the evolution of the spectral separation $\Delta\lambda$ between parts of the seed located at a distance $4\sigma_t$, as a function of σ_t, calculated by means of Eqs. 5 and 3. Two different values of the bandwidth have been considered, corresponding to the two limiting cases at FERMI@Elettra: for a seed energy per pulse below $10\,\mu$J, the spectral bandwidth is close to $\sigma_\lambda = 0.3$nm whereas, for higher energies and thus intensities, nonlinear effects can broaden the spectrum up to $\sigma_\lambda = 0.5$nm.

#191851 - $15.00 USD Received 6 Jun 2013; revised 19 Aug 2013; accepted 20 Aug 2013; published 19 Sep 2013
(C) 2013 OSA

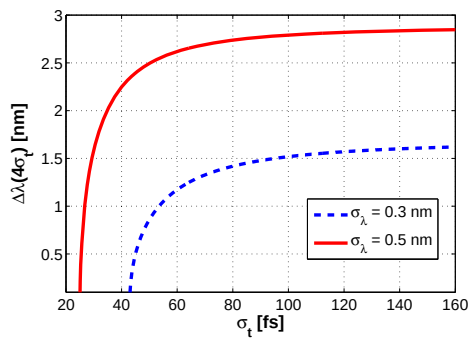

Fig. 4. Evolution of $\Delta\lambda(4\sigma_t)$ as a function of σ_t for the following bandwidths of the seed carrying a linear positive chirp: $\sigma_\lambda = 0.3$nm (dashed line) and $\sigma_\lambda = 0.5$nm (full line). These values correspond to limiting cases of accessible Gaussian spectra at FERMI@Elettra. For a negative chirp, one gets the same values of $\Delta\lambda(4\sigma_t)$, but with opposite sign. The σ_t corresponding to $\Delta\lambda(4\sigma_t) = 0$nm is the (theoretical) duration of a Fourier-transform limited pulse.

For increasing values of σ_t (i.e., for an increasing amount of chirp), $\Delta\lambda$ reaches an asymptotic value. Examining Fig. 4, one therefore sees for the case of FERMI@Elettra $\Delta\lambda$ is limited to about 3nm. This information is important because it sets an effective limit to the spectral separation $\Delta\lambda_n$ of the two pulses generated by the FEL.

Electron beam: energy chirp

As is now well known for CHG FEL's in which the electron beam acts as an intermediary in carrying the coherent seed signal, temporal variations such as chirps in the energy profile may seriously impact the FEL output emission (see, e.g., [22–26]). A linear electron beam energy chirp, whose slope will be noted κ_1, couples to the total chromatic dispersion of the dispersive section and downstream undulators resulting in a simple shift of the central wavelength of FEL emission [23]. In principle, any corresponding gain reduction due to this shift can be compensated by either retuning the resonant wavelength of the undulators (see Eq. 1) or by slightly adjusting the seed wavelength. However, a quadratic chirp component κ_2 will result in spectral broadening of output emission [24, 26] and, for sufficiently large magnitudes, can also reduce the FEL gain if the broadening becomes a significant fraction of the FEL's gain bandwidth. In principle, here too the effect can be compensated by placing an equal magnitude but negative chirp on the seed pulse [27]. In the context of the subject matter of this paper, namely the formation and control of a double spectro-temporal peak, a quadratic electron beam energy chirp can either enhance or reduce the spectral offset between the two peaks and thus must be carefully taken into account.

A simple linear and quadratic energy chirp can be modelled as:

$$E(t) = E_0 + \kappa_1 t + \kappa_2 t^2. \tag{7}$$

The exact amplitudes of the κ_1 and κ_2 coefficients at entrance to the FEL depend upon various propagation effects as the electron beam is transported through the linear accelerator (linac). First of all, the radio-frequency (RF) accelerating fields [28] of the successive linac sections (generally phased at or very close to crest) induce a negative quadratic chirp. Second, in order to increase the electron beam current (and thus enhance the FEL emission), the electron bunch

#191851 - $15.00 USD Received 6 Jun 2013; revised 19 Aug 2013; accepted 20 Aug 2013; published 19 Sep 2013
(C) 2013 OSA

is time-compressed. On FERMI@Elettra, this is done by first imposing a positive linear chirp component via phasing of two upstream linac sections off crest, and then by sending the electron beam through a magnetic chicane that converts the linear energy chirp into longitudinal compression. However, this procedure generates an additional negative curvature of the temporal energy profile. In order to linearize the longitudinal electron-beam phase space during the compression (generally necessary to have a relatively constant current profile), an X-band, 4th harmonic RF cavity [29] positioned just upstream of the chicane is run close to negative crest to provide a positive contribution to the κ_2 coefficient and compensate the aforementioned negative curvature. Following compression, strong longitudinal wakefields [30] in the downstream linac act upon the much higher current electron beam bunch: they induce a chirp that contains both a linear, negative term and a positive curvature component. While the linear κ_1 coefficient can be eliminated by slightly dephasing off crest the last couple RF linac sections (at a price of a small reduction in final beam energy), there is no simple way to reduce the quadratic κ_2 coefficient and therefore in general the electron beam enters the FEL with a quadratic energy chirp.

At FERMI@Elettra, we characterize the electron beam longitudinal phase space at the end of the linac via a diagnostic section composed of an RF deflecting cavity [31] followed by an energy spectrometer. The cavity stretches the beam in the vertical direction, inducing a correlation between the temporal distribution and the vertical displacement. The bending magnet chromatically disperses the electrons in the horizontal plane, making the information about the beam energy profile available along that direction. The beam longitudinal phase space can then be visualized on a fluorescent YAG crystal + CCD camera system placed downstream, as shown in Fig. 5. This particular $E(t)$ distribution corresponds to the configuration in which most of the results presented in this paper have been obtained. The energy profile is very close to a parabola with a quite small linear component (i.e., $\kappa_1 \approx 1\,\text{Mev/ps}$) and a much more significant quadratic component with $\kappa_2 \approx 7\,\text{Mev/ps}^2$. In Section 4 we consider the impact of this quadratic component upon double peak formation.

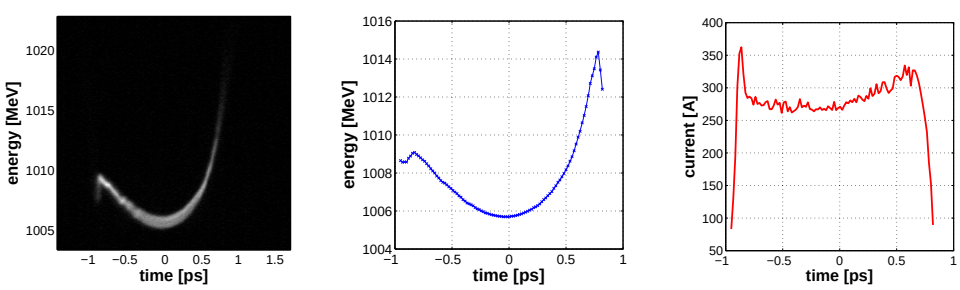

Fig. 5. Electron beam longitudinal phase space measured at the RF deflector/spectrometer diagnostic end station of the FERMI@Elettra linac. Left: raw CCD spectrometer image; center: energy profile determined from image analysis; right: current profile. Here time *increases* from the beam head to the beam tail.

As shown in the right panel of Fig. 5, the current profile is almost flat in the middle of the bunch, even if a slow ramp towards the tail can be noticed. Experimentally, there is a typical shot-to-shot jitter of $\approx 50\,\text{fs}$ of the relative electron beam-seed timing. This jitter in conjunction with current inhomogeneities results in a fluctuation of the FEL power, as the seed "explores" different temporal portions of the beam. This effect may be relevant for user applications but does not affect the formation of the spectro-temporal double peak.

We now give a quantitative description of the two-colour emission results at FERMI@Elettra.

#191851 - $15.00 USD Received 6 Jun 2013; revised 19 Aug 2013; accepted 20 Aug 2013; published 19 Sep 2013
(C) 2013 OSA

3. Experimental results

Figure 6 shows the behaviour of the FEL spectrum at the 6th harmonic of the seed (43.5 nm) as one sweeps the relative time delay between the seed and the electron beam. To the best of our knowledge, this picture provides the first direct *experimental* evidence of the temporal pulse splitting in an FEL due to local overbunching induced by an intense seed. At a delay ≈ -0.8 ps, the seed is superimposed on the electron beam tail, so that the first peak (at larger wavelength, since the frequency chirp is positive) appears. Then, at a delay ≈ -0.6 ps, the whole seed pulse lies on top of sufficiently high current portions of the electron beam and the second peak (at shorter wavelength) also appears.

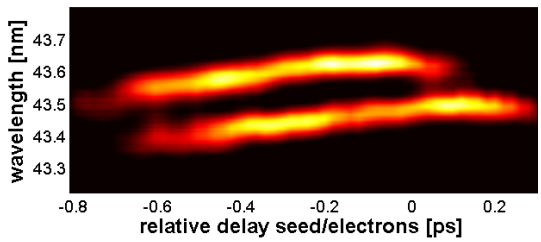

Fig. 6. FEL spectrum at the 6th harmonic of the seed (43.5 nm), as a function of the relative delay between the seed pulse and the electron beam. At the zero value of the delay, the seed pulse is approximately centered on the bunch of electrons. The dispersive section R_{56} and seed energy were set, respectively, to 23 μm and 80 μJ; see Table **??** for other parameters.

As we remarked in the previous section, a linear energy chirp of the electron energy induces a spectral shift of the FEL emission. Hence, when they appear near the tail portion of the electron beam, both peaks are detuned towards shorter wavelengths because of the strong local negative slope of the electron beam chirp (see Fig. 5). For smaller relative timing delays (i.e., moving the seed from overlapping the tail toward the head of the bunch), the central wavelengths of the two peaks drift redward due to the increase of the value of the local linear chirp of the electron energy distribution. However, the separation between the two spectral peaks ($\Delta\lambda_6 \approx 0.17$ nm), their relative heights and their respective widths remain practically constant. The wavelength drift flattens out about 100 fs before the first spectral peak disappears; this behaviour is mirrored 200 fs later in the second peak. This early disappearance might be caused by the small current ramp from the center of the bunch to its tail (see Fig. 5) and/or by degraded transverse properties in this region.

In this experiment, the external seed chirp was created both during the propagation through different optical components such as lenses and windows, and by self-phase modulation due to high intensity. We typically measured a seed bandwidth $\sigma_\lambda \approx 0.45$ nm and a duration $\sigma_t \approx$ 90 fs (determined by cross-correlating the seed pulse with an infrared pulse, extracted from the oscillator of the Ti:Sapphire laser chain, whose FWHM duration ≈ 80 fs). This gives $\Gamma_i \approx 6.2 \cdot 10^{-5}\,\mathrm{fs}^{-2}$, leading to the retrieval of the theoretical separation between the two sub-pulses, defined in Section 2. From Eqs. 5 and 6, we obtain:

$$\Delta t = \frac{\Delta\omega}{2\Gamma_i} = \frac{n\pi c}{\Gamma_i \lambda^2} \cdot \Delta\lambda_n, \tag{8}$$

where c is the speed of light. For an harmonic order $n = 6$, $\Delta t \approx 230$ fs (equal to $2.5\sigma_t$). The accuracy of this result will in principle be affected by the intrinsic chirp induced in the radiation during the FEL process [32] and by any quadratic energy chirp on the electron bunch. However,

#191851 - $15.00 USD Received 6 Jun 2013; revised 19 Aug 2013; accepted 20 Aug 2013; published 19 Sep 2013
(C) 2013 OSA

the size of the former is usually quite small relative to other chirps and the contribution of the latter is minor for our conditions, as will be confirmed in Section 4.

Up to now, we mainly focused on the effect of the seed power upon double spectro-temporal pulse formation. However, other parameters can influence the production and separation of the peaks. One is the strength of the dispersive section, as already discussed in [13] and experimentally demonstrated here in Fig. 7(a). Indeed, the dispersive section has an effect very similar to that of the seed power: the higher its strength, the lower the required seed power to produce a double pulse. Some small differences in the trend may be observed essentially because changing the seed intensity may affect the non-linear optical material dispersion and thus the chirp, while this does not happen when the R_{56} is varied. Similarly, when employing a strong dispersive section, a moderate seed power can be sufficient to increase the peaks separation. Fig. 7(b) shows a different way to modify the spectral separation of the two pulses, i.e., by changing the seed chirp. However, increasing the seed chirp above a given limit does not produce any significant change in the FEL spectrum. This can be expected from the limitation of $\Delta\lambda$ shown in Fig. 4.

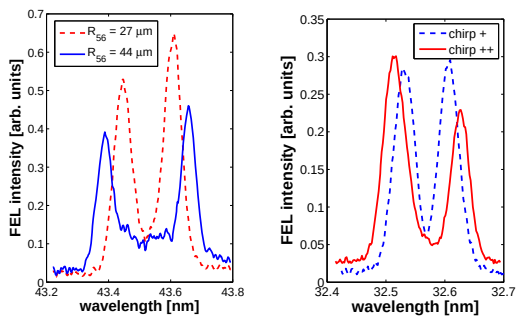

(a) (b)

Fig. 7. Observed double spectral peaks: (a) for two different strengths of the dispersive section and (b) for two different chirp values of the seed (b), corresponding to the standard positive chirp ("chirp +", $\sigma_\lambda \approx 0.45$ nm and $\sigma_t \approx 90$ fs with a seed energy of $\approx 70\,\mu$J) and a stronger chirp ("chirp ++", $\sigma_\lambda \approx 0.5$ nm and $\sigma_t \approx 160$ fs with a seed energy of $\approx 75\,\mu$J) induced by adding a piece of 50-mm thickness of CaF_2. For (b), the configuration of the machine was different than the one described in Table 1: 6 radiators were used, tuned to the 8th harmonic of the seed (32.6 nm), $R_{56} = 80\ \mu m$ and the electron beam had the following parameters: mean energy 1270 MeV, $\kappa_1 \approx 8$ MeV/ps, $\kappa_2 \approx 0.3$ MeV/ps^2, FWHM duration 2 ps, peak current ≈ 200 A.

Also the relative heights of the peaks can be easily controlled, favouring the growth of one over the other, by tuning the wavelength corresponding to FEL resonance of the undulators. The spectrum represented by the dotted line in Fig. 8 corresponds to a central tuning of the undulators. The data represented by the solid line were taken at slightly negative detuning; while both peaks can be seen, the one at shorter wavelength is significantly stronger. The dashed curve shows a situation where the detuning is positive, for which the peak of the gain curve has moved to longer wavelengths. Here the shorter wavelength pulse has been almost completely suppressed.

4. Simulations

The formation of the double peak is well reproduced by simulations [13] carried out using both 3D [33] and 1D numerical codes [34]. Figure 9 shows a comparison of the spectral pulse

#191851 - $15.00 USD Received 6 Jun 2013; revised 19 Aug 2013; accepted 20 Aug 2013; published 19 Sep 2013
(C) 2013 OSA

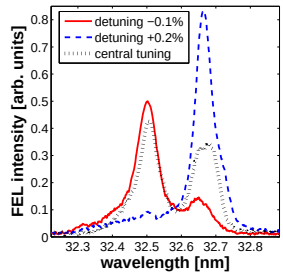

Fig. 8. Double peak for different tuning conditions of the radiators. The seed was in its standard configuration so that $\sigma_\lambda \approx 0.45$ nm and $\sigma_t \approx 90$ fs with an energy per pulse of $\approx 70\,\mu$J. The configuration of the rest of the machine was different than the one described in Table 1: 6 radiators were used, tuned to the 8th harmonic of the seed (32.6 nm), $R_{56} = 60\,\mu$m and the electron beam had the following parameters: mean energy 1175 MeV, $\kappa_1 \approx 0$ MeV/ps, $\kappa_2 \approx 10$ MeV/ps^2, FWHM duration 0.8 ps, peak current ≈ 600 A.

splitting between the experimental data and 1D Perseo code simulations. As it can be seen, the agreement is very satisfactory. Note that in the simulations, the relative power before splitting is slightly higher than the one measured experimentally. For running the simulations, we used typical values of measured seed and electron beam parameters, that are mentioned in the captions of Fig. 9, Fig. 10 and Fig. 11.

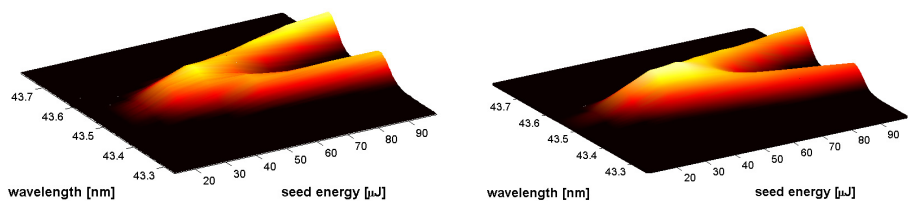

(a) experiment (b) simulations

Fig. 9. Comparison of the spectral splitting observed experimentally (a) and reproduced by simulations (b) using the code Perseo. For simulations, the following parameters were used for the electron beam: $\kappa_1 = 1$ MeV/ps, $\kappa_2 = 7$ MeV/ps^2, normalized transverse emittance 1 mm-mrad, relative energy spread 0.01%, peak current 300 A, average Twiss function $\beta = 10\,\mu$m. For each value of the seed energy, the bandwidth and the duration of the seed pulse were determined from interpolation of experimental values, growing linearly from $\sigma_\lambda = 0.35$ nm to $\sigma_\lambda = 0.45$ nm and from $\sigma_t = 70$ fs to $\sigma_t = 90$ fs as the seed energy increased from $10\,\mu$J to $100\,\mu$J. For other parameters, please refer to Table 1.

Let us now focus on one single measurement. Figure 10 shows the predicted spectrum and temporal profiles, obtained for simulation parameters that allow a good reproduction of the dashed-line spectrum reported in Fig. 7(a). The simulations have been carried out both for an ideal (i.e., flat in current and in energy) electron beam (dashed line), and the "real" electron-beam energy distribution shown in Fig. 5 (solid line). As shown in the left panel of Fig. 10, the positions of the spectral peaks are similar for the two cases: a slight reduction of the pulse separation on the order of 0.01 nm can be observed in the "real" case. Such a small contribution may be neglected in our conditions and, in any case, the double peak formation is not affected. Moreover, if we calculate using Eq. 8 the theoretical separation between the two sub-pulses in

#191851 - $15.00 USD Received 6 Jun 2013; revised 19 Aug 2013; accepted 20 Aug 2013; published 19 Sep 2013
(C) 2013 OSA

the spectrum represented in Fig. 7(a), we find $\Delta t = 198\,\text{fs}$. This is close to the value found in the simulation (right panel of Fig. 10), that is $\Delta t = 186\,\text{fs}$. Therefore, we claim that the agreement between theoretical, experimental and numerical studies can be considered as very satisfactory.

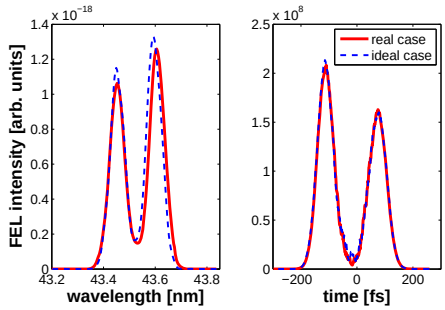

Fig. 10. Predicted FEL spectral and temporal profiles obtained using the the numerical code Perseo, for the following parameters: seed bandwidth $\sigma_\lambda = 0.47\,\text{nm}$, duration $\sigma_t = 93\,\text{fs}$, energy $70\,\mu\text{J}$ and central wavelength $261.1\,\text{nm}$; $R_{56} = 20\,\mu\text{m}$; electron beam peak current 300 A, normalized transverse emittance 1 mm-mrad, relative energy spread 0.01% and average Twiss function $\beta = 10\,\mu\text{m}$; undulators tuned to the 6th harmonic of the seed (43.5 nm). The dashed line represents the results obtained using an ideal, constant current, chirpless electron beam. The solid line shows simulation results for an electron beam with a current profile corresponding to Fig. 5 and energy chirps of 1 MeV/ps (linear) and 7 MeV/ps^2 (quadratic).

For this set of data, the spectral peaks have similar bandwidths $\sigma_\lambda \approx 0.028\,\text{nm}$, and the temporal pulses have similar durations, i.e., $\sigma_t \approx 30\,\text{fs}$. According to these numbers, the duration of each sub-pulse is ≈ 1.6 times greater than the Fourier-transform limit for a Gaussian spectrum. The distance from the Fourier-transform limit can be further reduced, e.g. by tuning the chirp of the seed laser. Since the seed and thus the FEL pulses are chirped, one could have expected a significant negative impact on the time-bandwidth product of each sub-pulse. However, this is not the case since each peak is quite narrow, and therefore barely sees the phase curvature of the seed electric field. Moreover, this also indicates that the phase of FEL pulses does not present high-order distortions.

Before concluding, let us consider a situation where the quadratic chirp of the electron beam is no longer negligible. We carried out simulations with same parameters as before for several values of quadratic chirp, but without any linear component (i.e., $\kappa_1 = 0\,\text{MeV/ps}^2$). In Fig. 11, we see that the value of κ_2 has almost no effect on the temporal shape of the FEL emission but that, as already stated in Section 2, the individual bandwidths and separation of the two spectral peaks are directly affected. Consequently, a quadratic energy chirp of the electron beam acts on the spectrum in a very similar way as does a linear chirp of the seed laser, and thus both may be used individually or in conjunction to modulate the spectral shape of the FEL emission.

Conclusion

We studied the mechanism leading to the generation of two spectrally- and temporally-separated radiation pulses for a seeded, harmonic upshift free-electron laser operating in the extreme ultra-violet spectral region. This mechanism, discovered and studied in detail at the FERMI@Elettra FEL facility, relies on the use of a high-power chirped seed pulse to produce strong, coherent overbunching in an electron beam; the presence of the chirp is the key element to producing a spectral splitting between the two temporal pulses. By changing either the seed laser power or the strength of the dispersive section, we demonstrated excellent control of both

#191851 - $15.00 USD Received 6 Jun 2013; revised 19 Aug 2013; accepted 20 Aug 2013; published 19 Sep 2013
(C) 2013 OSA

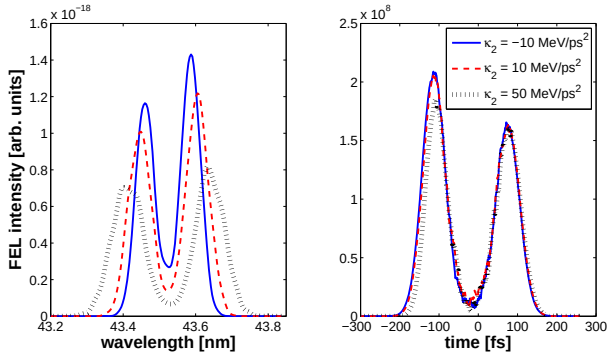

Fig. 11. Comparison of the outputs of simulations carried out with the numerical code Perseo for different values of the quadratic chirp of the electrons (left: spectrum; right: temporal intensity), for the following parameters: seed bandwidth $\sigma_\lambda = 0.47$ nm, duration $\sigma_t = 93$ fs, energy 70 μJ and central wavelength 261.1 nm; $R_{56} = 20\,\mu$m; undulators tuned to the 6th harmonic of the seed (43.5 nm); electron beam peak current 300 A, normalized transverse emittance 1 mm-mrad, relative energy spread 0.01%, average Twiss function $\beta = 10\,\mu$m and no linear chirp component. Solid line: $\kappa_2 = -10$ MeV/ps^2; dashed line: $\kappa_2 = 10$ MeV/ps^2; dotted line: $\kappa_2 = 50$ Mev/ps^2 .

the temporal distance and the spectral separation between the generated pulses. We also found that for our particular operation regime, the onset of the pulse splitting and the control of the pulses properties are only slightly affected by temporal variations in electron beam properties such as the current. Quadratic energy chirps do affect the spectral bandwidths and separation between the two pulses, but have negligible effect on their temporal separations. The temporal separation between pulses can be directly retrieved from the measurement of the FEL spectrum and from the knowledge of the seed chirp properties. Such an information can be extremely important when exploiting the two-pulse generation to carry out jitter-free, pump-probe user experiments. As a possible application of this configuration, we refer the interested reader to the recent work performed on the DIPROI beamline at FERMI@Elettra [11] and investigations of ultrafast magnetic processes [35].

Acknowledgments

We acknowledge the valuable contribution of the FERMI@Elettra commissioning and operations team. We also profited from insightful discussions with F. Bencivenga, C. Callegari, F. Capotondi and M. Labat. This work was funded by the FERMI@Elettra project of Elettra-Sincrotrone Trieste, partially supported by the Ministry of University and Research under grant numbers FIRB-RBAP045JF2 and FIRB-RBAP06AWK3. The work of B. Mahieu, G. De Ninno and D. Gauthier has been partially supported by the CITIUS project, funded by the Program for cross-border cooperation Italy-Slovenia 2007-2013. B. Mahieu is also grateful to the Egide agency and the Triangle de la Physique network for their financial support in the framework of, respectively, the XUV-FISCH and XUV-PhLAGH projects.